

REVEAL: Reasoning-enhanced Forensic Evidence Analysis for Explainable AI-generated Image Detection

Huangsen Cao, Qin Mei, Zhiheng Li, Yuxi Li, Ying Zhang, Chen Li, Zhimeng Zhang, Xin Ding, Yongwei Wang, Jing LYU and Fei Wu

Abstract—With the rapid advancement of generative models, visually realistic AI-generated images have become increasingly difficult to distinguish from authentic ones, posing severe threats to social trust and information integrity. Consequently, there is an urgent need for efficient and truly explainable image forensic methods. Recent detection paradigms have shifted towards explainable forensics. However, state-of-the-art approaches primarily rely on post-hoc rationalizations or visual discrimination, lacking a verifiable chain of evidence. This reliance on surface-level pattern matching limits the generation of causally grounded explanations and often results in poor generalization. To bridge this critical gap, we introduce **REVEAL-Bench**, the first reasoning-enhanced multimodal benchmark for AI-generated image detection that is explicitly structured around a chain-of-evidence derived from multiple lightweight expert models, then records step-by-step reasoning traces and evidential justifications. Building upon this dataset, we propose **REVEAL** (Reasoning-enhanced Forensic Evidence Analysis), an effective and explainable forensic framework that integrates detection with a novel expert-grounded reinforcement learning. Our reward mechanism is specially tailored to jointly optimize detection accuracy, explanation fidelity, and logical coherence grounded in explicit forensic evidence, enabling REVEAL to produce fine-grained, interpretable, and verifiable reasoning chains alongside its detection outcomes. Extensive experimental results demonstrate that REVEAL significantly enhances detection accuracy, explanation fidelity, and robust cross-model generalization, benchmarking a new state of the art for explainable image forensics.

Index Terms—AI-generated image detection, Explainable AI, Forensic reasoning.

1 INTRODUCTION

WITH the rapid evolution of generative artificial intelligence techniques such as Generative Adversarial Networks (GANs) [1, 2] and Diffusion Models [3], the visual realism of synthesized content has advanced to a level that can easily deceive human perception. While these advanced models have unlocked unprecedented creative and economic potential in fields like digital art, design, and film production, they have also raised significant concerns regarding misinformation, privacy violations, and copyright issues. The continual progress in advanced diffusion models such as FLUX [4] and SD3.5 [5], along with autoregressive generation methods (e.g., VAR [6]), has further intensified the challenge of distinguishing between real and synthetic content, making reliable detection an urgent research priority.

Recent research [7, 8, 9, 10, 11, 12] has made notable progress in detecting AI-generated images. However, most traditional methods focus solely on discrimination, offering limited forensic analysis. The emergence of multimodal large language models (MLLMs) offers new opportunities, enabling models to combine visual perception with textual descriptions. Recent endeavours such as GPT-4 based detection [13], AIGI-Holmes [14], FakeBench [15], and RAIDX [16] have initiated this transition towards explainability. Yet, as illustrated in Figure 2, these methods share fundamental limitations: they primarily rely on **post-hoc rationalizations** or leverage the MLLMs merely as a powerful general-purpose visual classifier to identify high-level visual anomaly patterns (e.g. “unnatural lighting”, “blurry edge”). They fail to construct a causally grounded **reasoning-based forensic pipeline** where specialized evidence is systematically collected, analyzed, and synthesized through logical deduction. Specifically, these prior works: 1) use datasets (e.g. FakeBench [15]) that lack **fine-grained, structured evidence**, limiting support for deep causal reasoning; and 2) rely on methods (e.g. RAIDX [16] with RAG) where

- Huangsen Cao, Qin Mei, Zhiheng Li, Zhimeng Zhang, Yongwei Wang, Fei Wu are with Zhejiang University. E-mail: huangsen_cao, yongwei.wang, wufei@zju.edu.cn.
- Yuxi Li, Ying Zhang, Chen Li, Jing Lyu are with WeChat Vision, Tencent Inc.
- Ding Xin is with Nanjing University of Information Science and Technology.

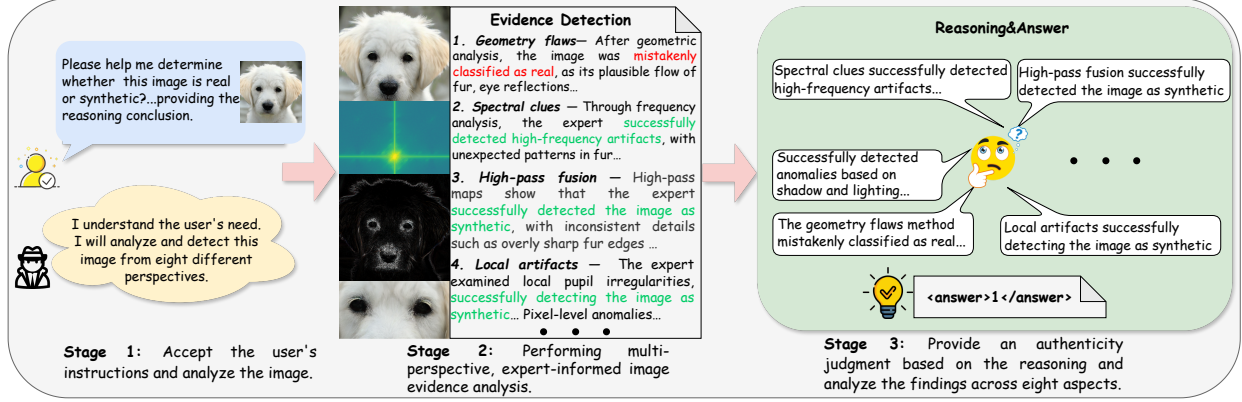


Fig. 1: Overview of the proposed REVEAL framework for reasoning-enhanced explainable synthetic image detection. The framework consists of three main stages: (1) receiving user instructions, (2) performing expert-grounded multi-perspective evidence detection, and (3) conducting reasoning through the chain of evidence (CoE) to derive a reliable decision with justifications.

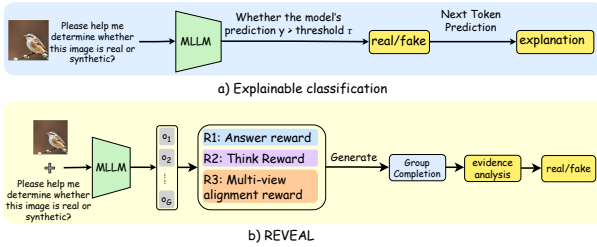


Fig. 2: a) Existing *post-hoc rationalization* detection. b) REVEAL framework, a *reasoning-enhanced* paradigm for truly explainable forensic analysis.

explanations exhibit **surface-level coherence** derived from pattern matching, rather than being grounded in verifiable forensic evidence traces.

The critical gap highlights two major challenges in developing reasoning-enhanced synthetic image detection: 1) Lack of a reasoning-oriented forensic dataset. Existing datasets contain either binary labels or shallow textual justifications, without structured and rigorous chain-of-evidence annotations necessary to build auditable forensic judgments. 2) Limited reasoning-based explainability. Current MLLM-based detectors tend to produce post-hoc rationalizations instead of verifiable reasoning chains, leading to fragile generalization and unreliable claims in the forensic context.

To this end, we introduce REVEAL-Bench, a novel reasoning-oriented benchmark for AI-generated image forensics. Our data generation pipeline is fundamentally distinct from existing approaches: we shift from general visual correlation to expert-grounded evidence analysis. For each image, we first leverage eight lightweight expert models to provide structured, reliable, low-level forensic evidence. Such evidence then forms the input for a subsequent large model

to generate a chain-of-evidence (CoE) annotation. By consolidating the multi-round forensic analysis from these specialized experts into a single, structured CoE trace, REVEAL-Bench becomes the first dataset to explicitly provide an expert-grounded, verifiable forensic analysis that connects low-level cues to high-level conclusions.

Building upon this dataset, we propose the REVEAL framework, a two-stage training paradigm designed to enforce reasoning-based forensic evidence analysis. In the first stage, we employ a supervised fine-tuning (SFT) to teach the MLLM the canonical CoE structure. In the second stage, we introduce R-GRPO (Reasoning-enhanced Group Relative Preference Optimization), an expert-grounded policy optimization algorithm, featuring a novel reward function critical for enhancing the logical coherence and verifiability of forensic analysis. Specifically, R-GRPO jointly optimizes (i) detection accuracy, (ii) reasoning stability, and (iii) multi-view consistency. The novel optimization enforces the MLLM to perform logical synthesis over explicit forensic evidence rather than simple visual pattern matching, thereby achieving accurate, reliable, and explainable forensic analysis.

In summary, our work makes three major contributions:

REVEAL-Bench. We pioneer the first reasoning-based and explainable dataset for AI-generated image detection. Unlike prior datasets that offer only post-hoc explanations, REVEAL-Bench is uniquely structured around expert-grounded, verifiable forensic evidence that embeds an explicit chain-of-evidence following a systematic evidence-then-reasoning paradigm.

REVEAL Framework. We introduce the REVEAL Framework, a progressive two-stage training

paradigm designed to instill standardized and explainable reasoning in multimodal LLMs. Its core, R-GRPO, optimizes the MLLM to perform logical synthesis for forensic evidence, jointly enhancing accuracy, reasoning consistency, and generalization.

Empirical Performance. Our approach achieves superior detection accuracy, generalization, and explanation fidelity, benchmarking a new state of the art for reasoning-based forensic research.

2 RELATED WORK

Detection of AI-Generated Fake Images: The rapid evolution of generative models, e.g., GANs [17, 18], autoregressive models [19], diffusion-based models [20, 21, 22, 23, 24, 25], has driven AI-generated images to near-photorealistic quality, challenging conventional detection methods. Early forensic studies focused on traditional manipulations like splicing or copy-move, analyzing noise inconsistencies, boundary anomalies, or compression artifacts [26, 27]. Researchers then shifted focus to generation artifacts, such as up-sampling grid effects, texture mismatches, or abnormal high-frequency decay [28, 29, 30]. For example, the Spectral Learning Detector [31] models the spectral distribution of authentic images, treating AI-generated samples as out-of-distribution anomalies, achieving consistent detection across generators. However, as generators incorporate post-processing techniques like super-resolution, these low-level statistical clues become increasingly subtle and less reliable for robust detection.

Recent methods employ general-purpose feature extractors, such as CNN- or ViT-based detectors, to learn discriminative features directly. While lightweight CNNs achieve strong benchmark performance [32], methods like the Variational Information Bottleneck (VIB) network [33] aim to enhance generalization by constraining feature representations through the information bottleneck principle to retain only task-relevant information. Post-hoc Distribution Alignment (PDA) [34] attempts to improve robustness to unseen generators by aligning regenerated and real distributions to detect unseen generators. Recently, NPR [12] has become a representative approach by capturing low-level artifacts, demonstrating strong generalization capability. Similarly, HyperDet [35] and AIDE [36] achieve robust generalization through high-frequency spectrum analysis. Despite their discriminatory power, these approaches remain limited in forensic value, as their conclusions rely on global statistics and lack the semantic, verifiable evidence required for comprehensive explainability.

Explainable AI-generated Image Detection: The emergence of MLLMs [37, 38] has accelerated the development of explainable image forensics by

leveraging their advanced cross-modal understanding [39, 40]. Early efforts reformulated detection as a Visual Question Answering (VQA) task [13, 41, 42], allowing MLLMs to provide accompanying descriptive text. FatFormer [11] extended this with a forgery-aware adapter to improve generalization on the CLIP-ViT [43] encoder.

Subsequent studies focused on constructing task-specific multimodal datasets for fine-tuning. FakeBench [15] and LOKI [44] provide synthetic images with manually written, high-level forgery descriptions. Holmes-Set [14] utilized small models for initial image filtering and a Multi-Expert Jury mechanism to generate post-hoc explanatory texts. At the methodological level, FakeShield [45], ForgerySleuth [46], ForgeryGPT [47] and SIDA [48] fine-tune MLLMs to achieve explainable forgery detection and localization. AIGI-Holmes [14] integrates low-level visual experts with reasoning modules. RAIDX [16] combines retrieval-augmented generation (RAG) [49] with GRPO optimization to improve the ability to describe texts.

Critically, existing datasets and methods suffer from two key limitations: First, the explanations are attributed to post-hoc rationalizations, often relying on the MLLM’s general knowledge and visual classification capabilities, failing to achieve logical synthesis of specialized forensic evidence. Second, they lack structured, fine-grained forensic evidence required to support a verifiable causal link between low-level artifacts and the final forensic judgments.

3 REVEAL-BENCH

As illustrated in Figure 3, this study constructs the REVEAL-Bench dataset through a rigorous, three-stage pipeline designed for reasoning-based image forensic: Data Curation & Pre-filtering, Expert-grounded Evidence Collection, and Chain-of-Evidence (CoE) Synthesis. This approach is fundamentally distinct as it replaces manual, subjective labeling with a process that systematically integrates verifiable evidence from specialized models with the logical synthesis capabilities of large vision-language models. The resulting dataset contains explicit, expert knowledge-grounded Chain-of-Evidence annotations, which is crucial for training forensic detectors with superior transparency and generalization capability.

Data Curation & Prefiltering: To ensure sufficient content, generator, and artifact diversity, we aggregate several prominent AI-generated detection benchmarks, including CNNDetection [7], UnivFD [10], AIGCDetectBenchmark [50], GenImage [51], Fake2M [52], and Chameleon [36]. This yielded in an initial corpus of approximately 5,120K synthetic

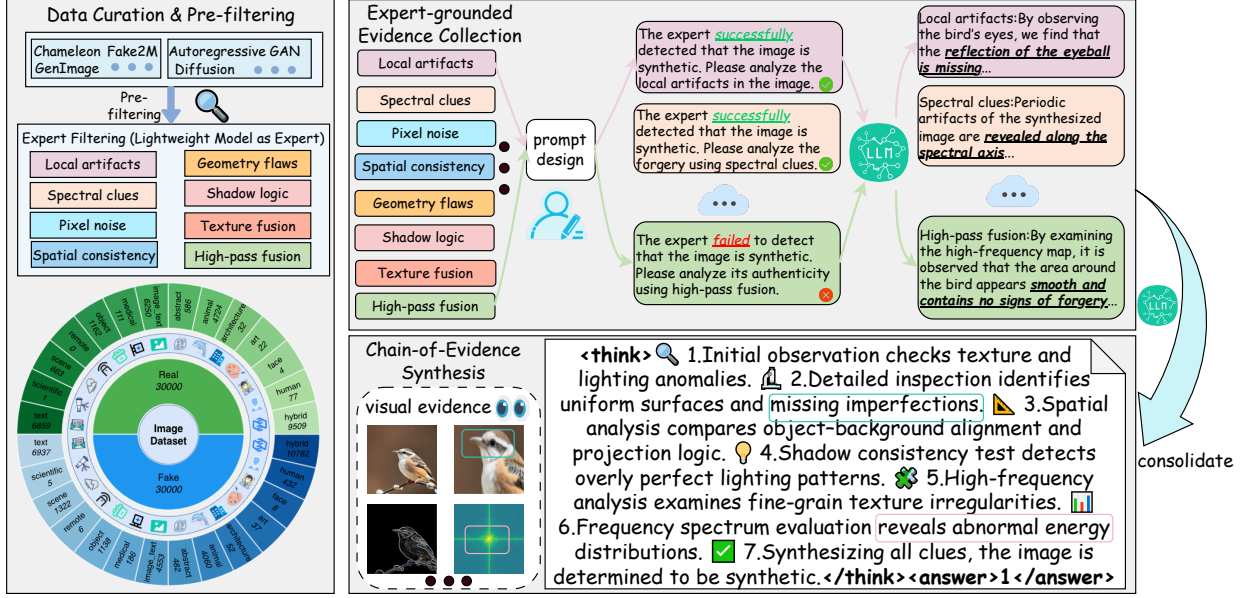


Fig. 3: **The pipeline of REVEAL-Bench.** This figure illustrates our data processing pipeline, which consists of three stages: Data Curation & Pre-filtering, Expert-grounded Evidence Collection, and Chain-of-Evidence (CoE) Synthesis

images and 850K authentic images. To manage annotation costs while ensuring high data quality, we implemented a stratified sampling strategy based on automated quality assessments [53] and image resolution. Specifically, we sampled images based on aesthetic scores (50% high, 30% medium, 20% low), and image resolution, high-resolution ($\geq 512 \times 512$) images at 50%, medium-resolution (384×384 – 512×512) images at 30%, and low-resolution ($< 384 \times 384$) images at 20%. Images were also semantically classified into 13 major categories (e.g., humans, architecture, artworks). After rigorous multi-stage filtering and preprocessing to eliminate non-representative or low-quality samples, we finalized a balanced corpus of 30K synthetic and 30K real images, which serves as the foundation for subsequent expert annotation

Expert-grounded Evidence Collection: To enable fine-grained, verifiable forensic analysis, we design and employ a set of eight lightweight and specialized expert models [54, 55, 12, 35, 56, 57], each dedicated to screening and localizing a distinct category of synthetic artifact (as depicted in Figure 3). This is a crucial distinction from prior work, such as AIGI-Holmes [14], which uses experts primarily for global filtering. Our experts, by contrast, provide *structured, machine-readable evidence*, including artifact masks and diagnostic labels. These eight outputs constitute the necessary **forensic evidence foundation**. By conditioning the LVLm on these high-fidelity, structured references, we ensure the final generated explanations are faithful, logically consistent, and ver-

ifiable against objective, low-level artifact data. This expert-grounded compositional analysis effectively bridges the gap between small-model perception of artifacts and large-model logical reasoning.

Chain-of-Evidence Synthesis: As shown in Figure 3, after the specialized expert annotation, the initial eight rounds of multi-perspective diagnostic outputs are diverse and fragmented. To construct a unified and progressive reasoning dataset suitable for Chain-of-Thought (CoT) fine-tuning, we leverage a high-capacity LVLm (Qwen-2.5VL-72B [58]) to perform structured knowledge consolidation. This process reconstructs the diverse, specialized evidence into a single, cohesive, and auditable reasoning trace, formatted using a standard `<think>...</think>.<answer>...</answer>` structure.

Fundamentally distinct from existing datasets like AIGI-Holmes [14] and FakeBench [15], which merely provide generic explanations, REVEAL-Bench explicitly formalizes the link between low-level expert evidence and high-level judgments. This two-stage pipeline transforms the detection tasks into a reasoning task, offering coherent CoE annotations that enhance logical consistency, minimizing annotation noise, and support supervision paradigms with advanced reinforcement learning techniques to improve explanation fidelity and generalization.

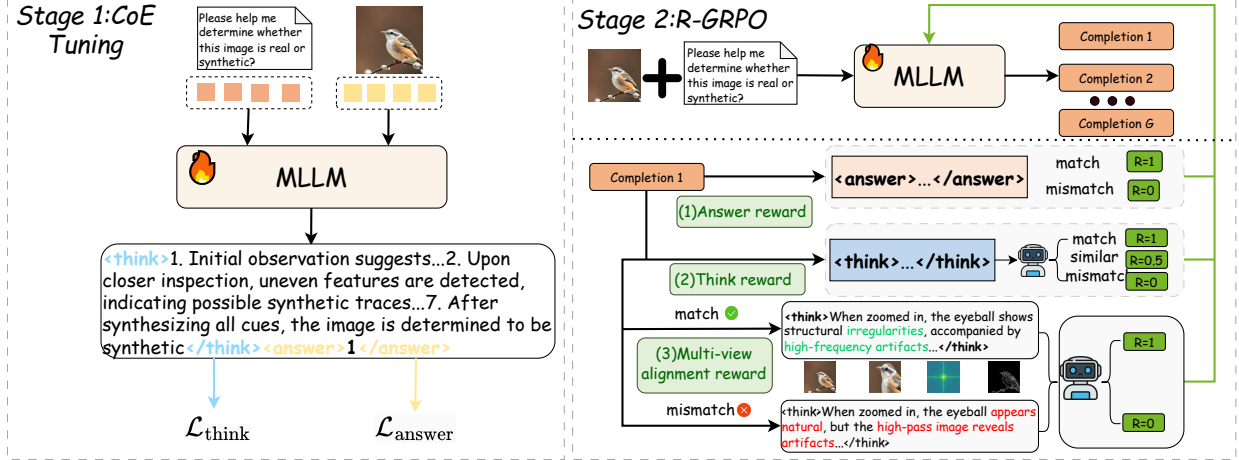


Fig. 4: Overview of REVEAL. The pipeline mainly consists of two stages: CoE Tuning and R-GRPO.

4 METHODOLOGY

4.1 Overview of REVEAL

As illustrated in Figure 4, the overall training pipeline adopts a two-stage progressive training paradigm inspired by advanced policy optimization-based reinforcement learning techniques [59].

We first perform supervised fine-tuning (SFT) on a consolidated Chain-of-Evidence (CoE) dataset to obtain a base policy that can deduce the required forensic reasoning procedure. While this stage establishes the fundamental reasoning-based forensic structure, the resulting model still exhibits limitations in logical consistency, forensic accuracy, and robustness. To mitigate these limitations, we propose a novel reinforcement learning algorithm: *Reasoning-enhanced Forensic Evidence Analysis* (R-GRPO). R-GRPO extends beyond standard Group Relative Policy Optimization (GRPO) by incorporating a task-specific composite reward that dynamically aligns forensic reasoning trajectories and stabilizes policy updates, significantly enhancing semantic consistency and reasoning robustness.

4.2 Progressive Multimodal Training for AI-Generated Image Detection

We introduce REVEAL (Reasoning-enhanced Forensic Evidence AnaLysis), a progressive multimodal training framework comprising two sequential stages designed to cultivate robust, logically consistent, and verifiable forensic reasoning in multimodal models.

Stage 1: Chain-of-Evidence Tuning (CoE Tuning). In the initial stage, we perform cold-start supervised fine-tuning to establish a stable, stepwise reasoning policy and a consistent output paradigm built upon the REVEAL-Bench dataset. Let x denote the visual input, $z = (z_1, \dots, z_T)$ denote the tokenized reasoning sequence (Chain-of-Evidence, CoE), and y denote the final classification label. We adopt an ex-

plicit joint reasoning–decision modeling paradigm, where the final prediction y is conditioned on the explicit reasoning trace z . This formulation enforces a **think-then-answer** mechanism, **fundamentally distinct from post-hoc rationalizations** (e.g. modeling $p(y | x)$ and then $p(z | x, y)$), thereby achieving causally grounded genuine explanations.

Concretely, we factorize the joint conditional probability as

$$p(y, z | x) = p(z | x) p(y | x, z), \quad (1)$$

which structurally encourages the model to first generate verifiable reasoning evidence and subsequently derive the final prediction conditioned directly on that reasoning process.

Maximizing the likelihood under (1) corresponds to minimizing the following negative log-likelihood loss:

$$\mathcal{L}_{\text{NLL}}(x, y, z; \theta) = -\log p_{\theta}(z | x) - \log p_{\theta}(y | x, z). \quad (2)$$

For training control and to explicitly balance the emphasis on reasoning quality versus final decision accuracy, we decompose \mathcal{L}_{NLL} into two components, the reasoning generation loss $\mathcal{L}_{\text{think}}$ and the answer loss $\mathcal{L}_{\text{answer}}$,

$$\mathcal{L}_{\text{think}} = -\sum_{t=1}^T \log p_{\theta}(z_t | z_{<t}, x), \quad (3)$$

$$\mathcal{L}_{\text{answer}} = -\log p_{\theta}(y | x, z), \quad (4)$$

We then employ a weighted composite SFT loss:

$$\mathcal{L}_{\text{SFT}} = (1 - \alpha) \mathcal{L}_{\text{think}} + \alpha \mathcal{L}_{\text{answer}} + \eta \text{KL}(\pi_{\text{pre}} \| \pi_{\theta}). \quad (5)$$

where $\alpha \in (0, 1)$ controls the relative importance of the answer loss versus the reasoning trace, the KL regularization term constrains the fine-tuned policy

π_θ to remain proximal to the pretrained policy π_{pre} , effectively mitigating catastrophic forgetting.

Stage 2: Reasoning-enhanced Group Relative Policy Optimization (R-GRPO).

Group Relative Policy Optimization (GRPO). Group Relative Policy Optimization (GRPO) is a reinforcement learning technique that stabilizes policy updates by comparing a group of candidate trajectories, rather than relying on the noisy reward signals of individual samples. Given an input x , we sample a group of K trajectories $\{\tau_i\}_{i=1}^K$ from the current policy π_θ , where each trajectory τ_i consists of an intermediate reasoning trace z_i and a final output y_i . A group-based composite reward $R_{\text{group}}(\tau_i)$ is computed for each trajectory, and the group-relative advantage A_i is defined by subtracting the mean group reward \bar{R}_{group} :

$$A_i = R_{\text{group}}(\tau_i) - \bar{R}_{\text{group}},$$

$$\bar{R}_{\text{group}} = \frac{1}{K} \sum_{j=1}^K R_{\text{group}}(\tau_j). \quad (6)$$

The GRPO objective maximizes the expected group-relative log-probability, regularized by a KL penalty for stable policy convergence:

$$\max_{\theta} \mathbb{E} \left[\sum_{i=1}^K A_i \log \pi_\theta(\tau_i | x) \right] - \lambda_{\text{KL}} \text{KL}(\pi_{\text{old}} \| \pi_\theta). \quad (7)$$

Reasoning-enhanced GRPO (R-GRPO). To employ GRPO for forensic analysis tasks, we propose *R-GRPO*, which augments the objective with a task-aware composite reward specifically designed to capture forensic fidelity and reasoning robustness. Let y denote the generated answer, y^* the reference answer, $z = (z_1, \dots, z_T)$ the reasoning tokens, and $\{v_m(x)\}_{m=1}^M$ a set of multi-visual visual evidence (e.g., spectral representations, high-pass filtered images, and localized artifact patches).

Rationale for Agent-based Reward Modeling. In preliminary experiments, we observed that simple metric-based rewards (e.g. using cosine similarity of sentence embeddings for r_{sem}) fail to adequately reflect the semantic and contextual logic required for high-quality forensic explanations. Therefore, we introduce a dedicated large language model as an intelligent agent (*Agent*) to evaluate responses. This Agent-based assessment considers contextual logic, explanation coherence, and factual consistency against the provided structured evidence, thereby generating a more human-aligned and interpretable reward signal than purely metric-based approaches (see Appendix A for details).

R-GRPO defines three complementary, evidence-driven reward components:

(1) *Answer Reward r_{sem} .* This binary reward ensures the accuracy of the detection:

$$r_{\text{sem}}(y, y^*) = \begin{cases} 1, & \text{if } y = y^*, \\ 0, & \text{otherwise.} \end{cases} \quad (8)$$

(2) *Think Reward r_{think} .* This reward quantifies the quality and structural integrity of the reasoning trace z .

Let $z = (z_1, \dots, z_T)$ be the generated reasoning trace and $z^* = (z_1^*, \dots, z_{T^*}^*)$ the ground-truth reasoning trace (when available). Define a perturbed trace $\tilde{z} = \text{shuffle}(z)$. Then

$$r_{\text{think}}(z, z^*, \tilde{z}) = \mathcal{A}_{\text{sem}}(z, z^*) + \mathcal{A}_{\text{logic}}(z, \tilde{z}), \quad (9)$$

where \mathcal{A}_{sem} measures alignment between the generated and reference reasoning, and $\mathcal{A}_{\text{logic}}(z, \tilde{z})$ evaluates the logical coherence of the trace. Crucially, $\mathcal{A}_{\text{logic}}$ evaluates the logical coherence by penalizing the model if minor structural perturbations \tilde{z} severely alter the inferred conclusion. This mechanism forces the model to maintain sequential consistency and ensure the reasoning steps are robustly connected.

(3) *Multi-view Alignment Reward r_{view} .* This reward encourages the generated reasoning trace z to be robustly grounded in evidence that persists across different forensic views of the image.

$$r_{\text{view}}(z, x) = \mathcal{A}_{\text{view}}\left(z, \{v_m(x)\}_{m=1}^M\right), \quad (10)$$

where $\mathcal{A}_{\text{view}}$ measures fidelity of the reasoning to the multi-view visual evidence $\{x_m\}$. By requiring alignment with evidence visible under different transformations (e.g., spectral, high-pass), this reward promotes cross-artifact generalization and enables the self-supervised discovery of novel, transformation-invariant artifacts.

The composite trajectory reward $R(\tau)$ combines these terms:

$$R(\tau) = \lambda_s r_{\text{sem}}(y, y^*) + \lambda_t r_{\text{think}}(z, z^*, \tilde{z}) + \lambda_v r_{\text{view}}(z, x), \quad (11)$$

where $\lambda_s, \lambda_t, \lambda_v \geq 0$ are tunable parameters balancing the rewards. For improved stability, rewards are standardized within each sampled group before calculating the advantage \hat{A}_i :

$$\hat{R}(\tau_i) = \frac{R(\tau_i) - \mu_{\text{group}}}{\sigma_{\text{group}}}, \quad (12)$$

$$\mu_{\text{group}} = \frac{1}{K} \sum_j R(\tau_j), \quad (13)$$

$$\sigma_{\text{group}} = \text{std}(\{R(\tau_j)\}) \quad (14)$$

and the normalized group-relative advantage is

$$\hat{A}_i = \hat{R}(\tau_i) - \frac{1}{K} \sum_j \hat{R}(\tau_j). \quad (15)$$

Unified GRPO with the R-GRPO objective. Combining the original GRPO formulation (7) with the R-GRPO composite reward (11), the unified optimization objective becomes

$$\max_{\theta} \mathbb{E} \left[\sum_{i=1}^K \hat{A}_i \log \pi_{\theta}(\tau_i | x) \right] - \lambda_{\text{KL}} \text{KL}(\pi_{\text{old}} \| \pi_{\theta}), \quad (16)$$

where \hat{A}_i encodes both the group-relative comparison and the reasoning-enhanced composite reward.

This evidence-enhanced reward signals can effectively guide the model to optimize its reasoning trajectories, enforcing both stability and logical coherence in verifiable forensic evidence analysis.

5 EXPERIMENTS

5.1 Experimental Settings

TABLE 1: Comparison of REVEAL-bench with previous datasets. REVEAL-bench is the first reasoning dataset for synthetic image detection.

Dataset	#Image	Explanation	Multiview Fusion	Reasoning Process
CNNDetection[7]	720k	✗	✗	✗
GenImage[51]	1M	✗	✗	✗
FakeBench[15]	6K	✓	✗	✗
Holmes-Set[14]	69K	✓	✓	✗
REVEAL-bench	60K	✓	✓	✓

To comprehensively evaluate the performance of REVEAL, we conduct experiments on two datasets: REVEAL-Bench and GenImage [51] (see Table 1). REVEAL-Bench, the first chain-of-evidence-based explainable dataset for synthetic image detection, serves as the in-domain dataset for training and evaluation. GenImage, a large-scale synthetic image dataset containing images generated by multiple generation methods, is used as an out-of-domain dataset to assess generalization. We train REVEAL on REVEAL-Bench and systematically evaluate its performance on both datasets (see Appendix B for detailed training settings). Building on this evaluation setup, we further investigate several core aspects of REVEAL’s capabilities. In particular, we study the impact of different MLLMs used as vision–language backbones, conduct ablation experiments to quantify the contribution of R-GRPO, and assess the model’s robustness under diverse perturbation settings. Appendix C reports the few-shot training results, and Appendix D provides a systematic comparison with existing large-scale model-based detectors.

Baselines We compare REVEAL with state-of-the-art AI-generated image detection methods, including CNNSpot [7], UnivFD [10], NPR [12], HyperDet [35], AIDE [36] and VIB-Net [60]. To ensure a fair comparison, we retrain these methods using the official code under the same experimental settings and datasets.

Evaluation metrics Following existing research, we adopt Accuracy (ACC) as our evaluation metric. Accuracy is defined as the proportion of correctly predicted samples among the total number of samples, reflecting the overall correctness of a classification model. Since our detection results are provided by the MLLM in textual form (Real/Fake), we convert these texts into binary labels to compute accuracy, while baseline methods use the default thresholds provided by their official code. Moreover, because the output of the MLLM is interpretable text rather than logit values, we do not consider metrics that require logit values for computation, such as Average Precision (AP), in our evaluation.

5.2 Generalization across datasets

Table 2 reports the performance of REVEAL on the in-domain dataset **REVEAL-bench** and the out-of-domain benchmark **GenImage**. The results indicate that REVEAL, leveraging a Chain-of-Evidence (CoE) reasoning-and-forensics mechanism, achieves superior cross-domain generalization compared to baseline lightweight binary classifiers: it maintains higher accuracy and more stable performance on GenImage. In the in-domain setting, smaller classifiers, such as those using methods like NPR[12] and AIDE[36], are more prone to overfitting, demonstrating stronger fitting ability to domain-specific statistical regularities and subtle signals. As a result, REVEAL’s performance in-domain is comparable to that of these compact models. However, REVEAL excels in terms of cross-domain generalization. These findings suggest that while smaller models remain attractive for tasks prioritizing computational efficiency and in-domain accuracy, REVEAL better preserves and propagates key reasoning cues across domains. Therefore, there is a clear trade-off between generalization and domain-specific fit that should inform deployment choices. Notably, in the context of synthetic-image detection, reasoning-based forensic approaches, like REVEAL, exhibit particularly robust generalization.

5.3 Generalization across Base MLLMs

The proposed algorithm in this study demonstrates strong generalizability and can be flexibly applied to a variety of multimodal large model architectures. To validate the effectiveness of our method, we conduct experiments using Qwen2.5-VL [58], LLaVA-1.5-VL [37], and Phi-3.5 as representative training frameworks. As shown in Table 3, the results indicate that our approach achieves excellent detection performance and robust generalization across different multimodal large models.

Furthermore, we observe that as the model size increases, the detection capability improves significantly. This trend suggests the existence of a scaling

TABLE 2: REVEAL demonstrates superior generalization across both in-domain and out-of-domain evaluations. REVEAL outperforms the best competing method by **3.87 %**.

Method	REVEAL-bench	Midjourney	SD v1.4	SD v1.5	ADM	GLIDE	Wukong	VQDM	BigGAN	Mean
CNNSpot [7]	87.80	62.45	74.25	73.85	63.55	73.60	73.70	71.35	39.45	68.89
UnivFD [10]	86.95	75.00	84.35	80.95	85.50	71.75	82.00	80.70	88.45	81.74
NPR [12]	95.40	<u>84.80</u>	88.85	88.05	85.10	94.30	87.05	84.45	88.95	88.55
HyperDet [35]	93.25	68.40	91.85	92.30	100.0	67.05	89.20	80.45	57.65	82.24
AIDE [36]	95.25	79.90	<u>95.90</u>	<u>94.95</u>	87.75	<u>90.35</u>	<u>94.85</u>	<u>90.10</u>	<u>91.10</u>	<u>91.13</u>
VIB-Net [60]	67.05	53.25	60.25	57.85	65.00	68.55	60.85	52.55	38.00	58.15
REVEAL	<u>95.31</u>	93.75	97.81	97.19	<u>95.00</u>	86.88	96.25	95.94	96.88	95.00

TABLE 3: Performance across different MLLMs, showing larger models exhibit consistently stronger detection capability.

Training Scheme	Phi-3.5	Qwen2.5-VL-3b	Qwen2.5-VL-7b	llava-v1.5-7b	llava-v1.5-13b
CoE Tuning	83.75	87.18	85.73	91.56	93.06
CoE Tuning+G-GRPO	87.19	89.06	92.19	92.81	95.31

law for synthetic image detection within the context of large models, similar to other tasks in the large model domain. As multimodal models continue to grow, their ability to handle complex tasks such as synthetic image detection becomes increasingly effective, demonstrating a direct correlation between model scale and performance.

5.4 Ablation Studies

TABLE 4: Ablation study of the impact of CoE Tuning, GRPO, and R-GRPO on model accuracy on REVEAL-Bench.

CoE Tuning	GRPO	R-GRPO	Acc
✗	✗	✗	61.21
✓	✗	✗	85.73
✓	✓	✗	91.56
✓	✗	✓	95.31

We conducted ablation experiments to investigate the role of reasoning datasets in synthetic image detection. As shown in Table 4, we first evaluated the performance of models trained without reasoning data (i.e., non-Reasoning SFT) and compared them with models fine-tuned using reasoning data (i.e., CoE Tuning). Additionally, we tested the effects of applying simple GRPO and our proposed R-GRPO method on performance improvement. The experimental results demonstrate that reasoning datasets significantly enhance the performance of MLLMs in synthetic image detection, with models lacking reasoning data performing close to random levels. Moreover, applying G-GRPO further improved the performance, highlighting the critical role of R-GRPO in this task.

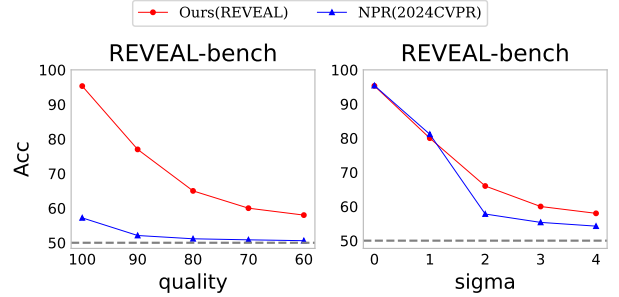


Fig. 5: The accuracy comparison between the two methods under various perturbation conditions.

5.5 Robustness Evaluation of REVEAL

To evaluate the robustness of REVEAL against common post-processing distortions, we conducted a systematic robustness study on the **REVEAL-bench** dataset. The experiments apply two typical post-processing operations to the original test images: Gaussian blur ($\sigma = 1, 2, 3, 4$) and JPEG compression (quality = 90, 80, 70, 60). For each distortion level, we compare REVEAL with the state-of-the-art baseline methods (results are shown in Figure 5). The results indicate that REVEAL demonstrates stronger robustness and improved cross-domain generalization across the considered post-processing settings.

6 CONCLUSION

We presented REVEAL, a reasoning-centered approach for explainable AI-generated image detection. First, we introduced **REVEAL-Bench**, the first dataset organized around expert-grounded, verifiable forensic evidence and an explicit chain-of-evidence following an evidence-then-reasoning paradigm. Second, we proposed the **REVEAL Framework**, a progressive two-stage training scheme whose core component R-GRPO explicitly teaches multimodal LLMs to perform logical synthesis over forensic evidence, jointly improving accuracy, reasoning consistency, and generalization. Empirically, REVEAL attains superior detection accuracy, stronger out-of-domain generalization, and higher explanation fidelity, establishing a new state of the art for reasoning-based image forensics.

REFERENCES

- [1] I. J. Goodfellow, J. Pouget-Abadie, M. Mirza, B. Xu, D. Warde-Farley, S. Ozair, A. Courville, and Y. Bengio, "Generative adversarial nets," *Advances in neural information processing systems*, vol. 27, 2014.
- [2] T. Karras, S. Laine, and T. Aila, "A style-based generator architecture for generative adversarial networks," in *Proceedings of the IEEE/CVF conference on computer vision and pattern recognition*, 2019, pp. 4401–4410.
- [3] P. Dhariwal and A. Nichol, "Diffusion models beat gans on image synthesis," *Advances in neural information processing systems*, vol. 34, pp. 8780–8794, 2021.
- [4] B. F. Labs, "Flux," <https://github.com/black-forest-labs/flux>, Jan 2024.
- [5] P. Esser, S. Kulal, A. Blattmann, R. Entezari, J. Müller, H. Saini, Y. Levi, D. Lorenz, A. Sauer, F. Boesel *et al.*, "Scaling rectified flow transformers for high-resolution image synthesis," in *Forty-first international conference on machine learning*, 2024.
- [6] K. Tian, Y. Jiang, Z. Yuan, B. Peng, and L. Wang, "Visual autoregressive modeling: Scalable image generation via next-scale prediction," *Advances in neural information processing systems*, vol. 37, pp. 84 839–84 865, 2024.
- [7] S.-Y. Wang, O. Wang, R. Zhang, A. Owens, and A. A. Efros, "Cnn-generated images are surprisingly easy to spot... for now," in *Proceedings of the IEEE/CVF conference on computer vision and pattern recognition*, 2020, pp. 8695–8704.
- [8] L. Chai, D. Bau, S.-N. Lim, and P. Isola, "What makes fake images detectable? understanding properties that generalize," in *European conference on computer vision*. Springer, 2020, pp. 103–120.
- [9] Z. Wang, J. Bao, W. Zhou, W. Wang, H. Hu, H. Chen, and H. Li, "Dire for diffusion-generated image detection," in *Proceedings of the IEEE/CVF International Conference on Computer Vision*, 2023, pp. 22 445–22 455.
- [10] U. Ojha, Y. Li, and Y. J. Lee, "Towards universal fake image detectors that generalize across generative models," in *Proceedings of the IEEE/CVF Conference on Computer Vision and Pattern Recognition*, 2023, pp. 24 480–24 489.
- [11] H. Liu, Z. Tan, C. Tan, Y. Wei, J. Wang, and Y. Zhao, "Forgery-aware adaptive transformer for generalizable synthetic image detection," in *Proceedings of the IEEE/CVF Conference on Computer Vision and Pattern Recognition*, 2024, pp. 10 770–10 780.
- [12] C. Tan, Y. Zhao, S. Wei, G. Gu, P. Liu, and Y. Wei, "Rethinking the up-sampling operations in cnn-based generative network for generalizable deepfake detection," in *Proceedings of the IEEE/CVF Conference on Computer Vision and Pattern Recognition*, 2024, pp. 28 130–28 139.
- [13] S. Jia, R. Lyu, K. Zhao, Y. Chen, Z. Yan, Y. Ju, C. Hu, X. Li, B. Wu, and S. Lyu, "Can chatgpt detect deepfakes? a study of using multimodal large language models for media forensics," in *Proceedings of the IEEE/CVF Conference on Computer Vision and Pattern Recognition*, 2024, pp. 4324–4333.
- [14] Z. Zhou, Y. Luo, Y. Wu, K. Sun, J. Ji, K. Yan, S. Ding, X. Sun, Y. Wu, and R. Ji, "Aigholmes: Towards explainable and generalizable ai-generated image detection via multimodal large language models," *arXiv preprint arXiv:2507.02664*, 2025.
- [15] Y. Li, X. Liu, X. Wang, B. S. Lee, S. Wang, A. Rocha, and W. Lin, "Fakebench: Probing explainable fake image detection via large multimodal models," *IEEE Transactions on Information Forensics and Security*, 2025.
- [16] T. Li, Z. Huang, H. Wen, Y. He, S. Lyu, B. Wu, and G. Cheng, "Raidx: A retrieval-augmented generation and grpo reinforcement learning framework for explainable deepfake detection," in *Proceedings of the 33rd ACM International Conference on Multimedia*, 2025, pp. 11 746–11 755.
- [17] I. Goodfellow, J. Pouget-Abadie, M. Mirza, B. Xu, D. Warde-Farley, S. Ozair, A. Courville, and Y. Bengio, "Generative adversarial networks," in *Advances in Neural Information Processing Systems*, vol. 3, 2014.
- [18] P. Esser, R. Rombach, and B. Ommer, "Taming transformers for high-resolution image synthesis," in *Proceedings of the IEEE/CVF Conference on Computer Vision and Pattern Recognition*, 2021, pp. 12 873–12 883.
- [19] A. Van Den Oord, O. Vinyals *et al.*, "Neural discrete representation learning," in *Advances in Neural Information Processing Systems*, vol. 30, 2017.
- [20] P. Esser, S. Kulal, A. Blattmann, R. Entezari, J. Müller, H. Saini, Y. Levi, D. Lorenz, A. Sauer, F. Boesel, D. Podell, T. Dockhorn, Z. English, K. Lacey, A. Goodwin, Y. Marek, and R. Rombach, "Scaling rectified flow transformers for high-resolution image synthesis," 2024.
- [21] J. Song, C. Meng, and S. Ermon, "Denoising diffusion implicit models," *arXiv preprint arXiv:2010.02502*, 2020.
- [22] J. Ho, A. Jain, and P. Abbeel, "Denoising diffusion probabilistic models," *arXiv preprint arXiv:2006.11239*, 2020.
- [23] S. Gu, D. Chen, J. Bao, F. Wen, B. Zhang, D. Chen, L. Yuan, and B. Guo, "Vector quantized diffusion model for text-to-image synthesis," in *Proceedings of the IEEE/CVF Conference on Computer Vision and*

- Pattern Recognition*, 2022, pp. 10 696–10 706.
- [24] C. Saharia, W. Chan, S. Saxena, L. Li, J. Whang, E. L. Denton, K. Ghasemipour, R. G. Lopes, B. K. Ayan, T. Salimans *et al.*, “Photorealistic text-to-image diffusion models with deep language understanding,” in *Advances in Neural Information Processing Systems*, vol. 35, 2022, pp. 36 479–36 494.
 - [25] Y. Ji, H. Yan, J. Lan, H. Zhu, W. Wang, Q. Fan, L. Zhang, and J. Zhang, “Interpretable and reliable detection of ai-generated images via grounded reasoning in mlms,” *arXiv preprint arXiv:2506.07045*, 2025.
 - [26] P. Zhou, X. Han, V. I. Morariu, and L. S. Davis, “Learning rich features for image manipulation detection,” in *Proceedings of the IEEE Conference on Computer Vision and Pattern Recognition*, 2018, pp. 1053–1061.
 - [27] H. Li, B. Wu, and Y. Sun, “Splicing localization via noise level inconsistency,” *IEEE Transactions on Image Processing*, 2022.
 - [28] J. Frank, T. Eisenhofer, L. Schönherr, A. Fischer, D. Kolossa, and T. Holz, “Leveraging frequency analysis for deep fake image recognition,” in *Proceedings of the 37th International Conference on Machine Learning*, 2020.
 - [29] Z. Liu, X. Qi, and P. H. Torr, “Global texture enhancement for fake face detection in the wild,” in *Proceedings of the IEEE/CVF Conference on Computer Vision and Pattern Recognition*, 2020, pp. 8057–8066.
 - [30] T. Dzanic, K. Shah, and F. D. Witherden, “Fourier spectrum discrepancies in deep network generated images,” in *Advances in Neural Information Processing Systems*, 2020.
 - [31] D. Karageorgiou, S. Papadopoulos, I. Kompatsiaris, and E. Gavves, “Any-resolution ai-generated image detection by spectral learning (spai),” in *Proceedings of the IEEE/CVF Conference on Computer Vision and Pattern Recognition*, 2025.
 - [32] L. Lađević, T. Kramberger, R. Kramberger, and D. Vlahek, “Detection of ai-generated synthetic images with a lightweight cnn,” *AI*, vol. 5, no. 3, p. 76, 2024.
 - [33] H. Zhang, Q. He, X. Bi, W. Li, B. Liu, and B. Xiao, “Towards universal ai-generated image detection by variational information bottleneck network,” in *Proceedings of the IEEE/CVF Conference on Computer Vision and Pattern Recognition*, 2025.
 - [34] L. Wang, W. Chen, Z. Li, and S. Guo, “Pda: Generalizable detection of ai-generated images via post-hoc distribution alignment,” *arXiv preprint arXiv:2502.10803*, 2025.
 - [35] H. Cao, Y. Wang, Y. Liu, S. Zheng, K. Lv, Z. Zhang, B. Zhang, X. Ding, and F. Wu, “Hyperdet: Generalizable detection of synthesized images by generating and merging a mixture of hyper loras,” *arXiv preprint arXiv:2410.06044*, 2024.
 - [36] S. Yan, O. Li, J. Cai, Y. Hao, X. Jiang, Y. Hu, and W. Xie, “A sanity check for ai-generated image detection,” *arXiv preprint arXiv:2406.19435*, 2024.
 - [37] H. Liu, C. Li, Q. Wu, and Y. J. Lee, “Visual instruction tuning,” *Advances in neural information processing systems*, vol. 36, pp. 34 892–34 916, 2023.
 - [38] P. Wang, S. Bai, S. Tan, S. Wang, Z. Fan, J. Bai, K. Chen, X. Liu, J. Wang, W. Ge *et al.*, “Qwen2-vl: Enhancing vision-language model’s perception of the world at any resolution,” *arXiv preprint arXiv:2409.12191*, 2024.
 - [39] T. Wu, K. Ma, J. Liang, Y. Yang, and L. Zhang, “A comprehensive study of multimodal large language models for image quality assessment,” in *European Conference on Computer Vision*. Springer, 2024, pp. 143–160.
 - [40] A. Talmor, J. Herzig, N. Lourie, and J. Berant, “Commonsenseqa: A question answering challenge targeting commonsense knowledge,” in *Proceedings of the 2019 Conference of the North American Chapter of the Association for Computational Linguistics: Human Language Technologies, Volume 1 (Long and Short Papers)*, 2019, pp. 4149–4158.
 - [41] M. Keita, W. Hamidouche, H. Bougueffa Eutamene, A. Taleb-Ahmed, D. Camacho, and A. Hadid, “Bi-lora: A vision-language approach for synthetic image detection,” *Expert Systems*, vol. 42, no. 2, p. e13829, 2025.
 - [42] Y.-M. Chang, C. Yeh, W.-C. Chiu, and N. Yu, “Antifakeprompt: Prompt-tuned vision-language models are fake image detectors,” *arXiv preprint arXiv:2310.17419*, 2023.
 - [43] A. Radford, J. W. Kim, C. Hallacy, A. Ramesh, G. Goh, S. Agarwal, G. Sastry, A. Askell, P. Mishkin, J. Clark *et al.*, “Learning transferable visual models from natural language supervision,” in *International conference on machine learning*. PmLR, 2021, pp. 8748–8763.
 - [44] J. Ye, B. Zhou, Z. Huang, J. Zhang, T. Bai, H. Kang, J. He, H. Lin, Z. Wang, T. Wu *et al.*, “Loki: A comprehensive synthetic data detection benchmark using large multimodal models,” *arXiv preprint arXiv:2410.09732*, 2024.
 - [45] Z. Xu, X. Zhang, R. Li, Z. Tang, Q. Huang, and J. Zhang, “Fakeshield: Explainable image forgery detection and localization via multimodal large language models,” *arXiv preprint arXiv:2410.02761*, 2024.
 - [46] Z. Sun, H. Jiang, H. Chen, Y. Cao, X. Qiu, Z. Wu, and Y.-G. Jiang, “Forgery sleuth: Empowering multimodal large language models for image manipulation detection,” *arXiv preprint arXiv:2411.19466*, 2024.

- [47] J. Liu, F. Zhang, J. Zhu, E. Sun, Q. Zhang, and Z.-J. Zha, "Forgerygpt: Multimodal large language model for explainable image forgery detection and localization," *arXiv preprint arXiv:2410.10238*, 2024.
- [48] Z. Huang, J. Hu, X. Li, Y. He, X. Zhao, B. Peng, B. Wu, X. Huang, and G. Cheng, "Sida: Social media image deepfake detection, localization and explanation with large multimodal model," in *Proceedings of the Computer Vision and Pattern Recognition Conference*, 2025, pp. 28 831–28 841.
- [49] P. Lewis, E. Perez, A. Piktus, F. Petroni, V. Karpukhin, N. Goyal, H. Küttler, M. Lewis, W.-t. Yih, T. Rocktäschel *et al.*, "Retrieval-augmented generation for knowledge-intensive nlp tasks," *Advances in neural information processing systems*, vol. 33, pp. 9459–9474, 2020.
- [50] N. Zhong, Y. Xu, S. Li, Z. Qian, and X. Zhang, "Patchcraft: Exploring texture patch for efficient ai-generated image detection," *arXiv preprint arXiv:2311.12397*, 2023.
- [51] M. Zhu, H. Chen, Q. Yan, X. Huang, G. Lin, W. Li, Z. Tu, H. Hu, J. Hu, and Y. Wang, "Gen-image: A million-scale benchmark for detecting ai-generated image," *Advances in Neural Information Processing Systems*, vol. 36, pp. 77 771–77 782, 2023.
- [52] Z. Lu, D. Huang, L. Bai, J. Qu, C. Wu, X. Liu, and W. Ouyang, "Seeing is not always believing: Benchmarking human and model perception of ai-generated images," *Advances in neural information processing systems*, vol. 36, pp. 25 435–25 447, 2023.
- [53] H. Talebi and P. Milanfar, "Nima: Neural image assessment," *IEEE transactions on image processing*, vol. 27, no. 8, pp. 3998–4011, 2018.
- [54] O. Li, J. Cai, Y. Hao, X. Jiang, Y. Hu, and F. Feng, "Improving synthetic image detection towards generalization: An image transformation perspective," in *Proceedings of the 31st ACM SIGKDD Conference on Knowledge Discovery and Data Mining V. 1*, 2025, pp. 2405–2414.
- [55] A. Sarkar, H. Mai, A. Mahapatra, S. Lazebnik, D. A. Forsyth, and A. Bhattad, "Shadows don't lie and lines can't bend! generative models don't know projective geometry... for now," in *Proceedings of the IEEE/CVF conference on computer vision and pattern recognition*, 2024, pp. 28 140–28 149.
- [56] C. Tan, Y. Zhao, S. Wei, G. Gu, P. Liu, and Y. Wei, "Frequency-aware deepfake detection: Improving generalizability through frequency space domain learning," in *Proceedings of the AAAI Conference on Artificial Intelligence*, vol. 38, no. 5, 2024, pp. 5052–5060.
- [57] J. Li, W. Jiang, L. Shen, and Y. Ren, "Optimized frequency collaborative strategy drives ai image detection," *IEEE Internet of Things Journal*, 2025.
- [58] S. Bai, K. Chen, X. Liu, J. Wang, W. Ge, S. Song, K. Dang, P. Wang, S. Wang, J. Tang *et al.*, "Qwen2. 5-vl technical report," *arXiv preprint arXiv:2502.13923*, 2025.
- [59] D. Guo, D. Yang, H. Zhang, J. Song, R. Zhang, R. Xu, Q. Zhu, S. Ma, P. Wang, X. Bi *et al.*, "Deepseek-r1: Incentivizing reasoning capability in llms via reinforcement learning," *arXiv preprint arXiv:2501.12948*, 2025.
- [60] H. Zhang, Q. He, X. Bi, W. Li, B. Liu, and B. Xiao, "Towards universal ai-generated image detection by variational information bottleneck network," in *Proceedings of the Computer Vision and Pattern Recognition Conference*, 2025, pp. 23 828–23 837.